# Kelvin-Helmholtz billows in rising morning inversions

# Kelvin-Helmholtz billows in rising morning inversions

**M A Kallistratova[1], I V Petenko[1,2], R D Kouznetsov[1,3], D D Kuznetsov[1], V S Lyulyukin[1] and V G Perepelkin[1]**

[1] A M Obukhov Institute of Atmospheric Physics RAS, Pyzhevskiy 3, 119017 Moscow, Russia
[2] Institute of Atmospheric Sciences and Climate, CNR, Via Fosso del Cavaliere 100, 00133, Roma, Italy
[3] Finnish Meteorological Institute, Erik Palmnin aukio 1, 00560 Helsinki, Finland

E-mail: lyulyukin@gmail.com

**Abstract.** Wavelike motions (similar to Kelvin-Helmholtz billows, KHBs) within the rising inversion layers during the morning transition of the atmospheric boundary layer (ABL) are investigated. The KHBs were depicted in sodar echograms obtained in a rural terrain near Moscow (Russia) in 2011. Power spectra of the intensity of the sodar return signal were calculated from inversion layers and from convective areas underneath. Comparison of the dominant spectral maximums for the inversion and convective parts of the ABL show connection between convective plumes and KHBs.

## 1. Introduction

In cloudless anticyclonic weather heating of the underlying surface beginning after sunrise leads to formation of an unstable stratification underneath the nocturnal inversion layer and to the lifting of this inversion layer (see, e.g. [1, 2, 3, 4]). Convection development process and morning rise of a surface radiation inversion are clearly visible in summer and winter time in the sodar echograms on Figs. 1(a) and 1(b), which were obtained in the beginning of 1980s at the Tsimlansk Scientific Station (Tsimla) and Zvenigorod Scientific Station (ZSS) of the A. M. Obukhov Institute off Atmospheric Physics. Incipient plume-shape signals characteristic for convection are seen beneath the rising turbulent layers. As seen in Fig. 1(a), the axis of low-level jet (LLJ) stream rises with the rise of the inversion layer, providing a significant wind shear within the layer.

The wavy structures in elevated inversion layers over the convection were reveald in the late 1960's with the help of radar and sodar [5, 6]. In recent years wave structures in rising inversions were also detected with lidar [7, 8]. Such structures like Kelvin-Helmholtz billows (KHBs) in form of "braids" are especially clearly visible on sodar echograms, examples of which are presented on Fig. 2. Quasi periods of the braids on Figs. 2(a) and 2(b) are quite different: 5–6 min and 45—50 sec accordingly. A similar visualization of distinct KHBs with periods of 6.0–6.5 min within elevating inversion layers was presented in [9] as well.

In this paper parameters of KHBs observed during morning transitions are described, and their connections with the wind shear and convective plumes are analyzed based on a spectral analysis of the sodar and related measurements data obtained in 2011 at ZSS.

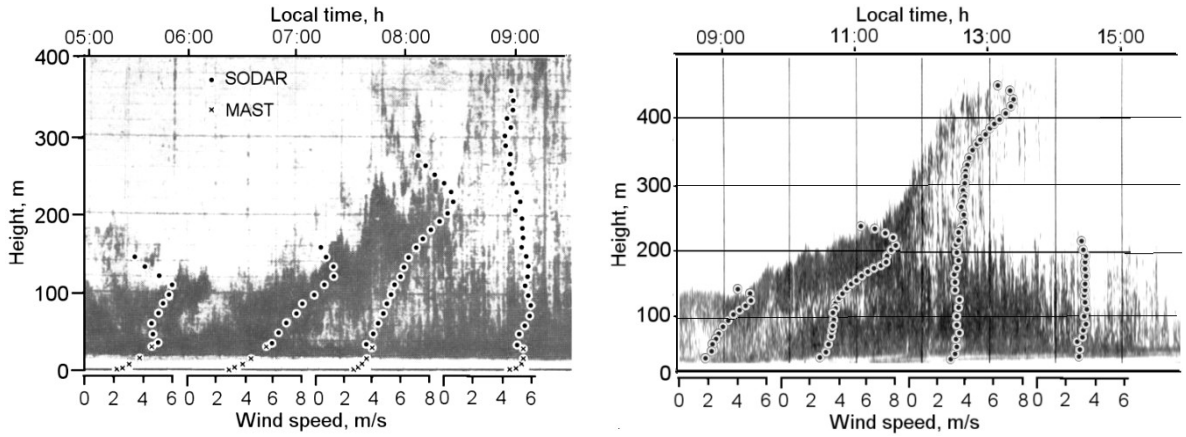


**Figure 1.** Examples of the sodar visualization of the rise of morning inversion heights. Dark areas of the echograms represent height-time intervals of strong echo returns. The 20-min averaged wind speed profiles are superimposed on the echograms. (a) TsSS (near Rostov, Russia), 15 July 1981; Sunrise was at 04:40. (b) ZSS (near Moscow, Russia), 23 Feb 1984; Sunrise was at 07:37.

## 2. Hypotheses on wave generation in stable layers above convection

The wave character of the sodar echo gives rise to many questions. Under what conditions these waves observed in the rising inversion, and under what conditions do they not appear? What is the nature of the interaction between the wavy motions within the rising inversion layers and the convective plumes under the layers. Are the KHBs generated by the convective plumes, or are the plumes modulated by the KHBs, or are they independent? What factors determine the duration of the rise and its height? Despite the fact that the study of waves in the stable layers over the convection continues about a half of century, there is no universally accepted answer to these questions.

In many publications the question about the waves sources is only posed without any answer (see e.g. [12, 13]). Other works (theoretical and experimental) include quite different hypothesis. We can distinguish three main hypotheses (or, more exactly, conjectures).

**Hypothesis A:** The waves are excited by the convection from beneath. It is the most widespread suggestion which is supported in publications [14, 15, 16, 17, 18, 7].

**Hypothesis B:** The waves are exited by internal gravity waves (IGWs) propagating in the middle and upper troposphere (e.g. by orographic waves). In other words the wave generation resulted from the passage, at relatively high speeds, of mesoscale waves, which perturbed the stability of the very nearly unstable boundary-layer shear flow in the course of their propagation. Sometimes such waves are defined as "ducted waves". Such suggestion is supported by Chimonas (1972) [19] and Hooke et al (1973) [20], and is partly assumed in Gossard et al (1971) [15] and Chimonas (1999) [21].

**Hypothesis C:** Waves in the rising inversion layer exist always due to the shear instability. However, not always can they be revealed due to restricted resolution of the measuring devices. Besides, the wave trains can pass aside over the measurement, thus not all of them can be depicted. The convective plums beneath the rising layers may serve as a trigger for the wave excitation. Such a hypothesis is supported in Reading et al (1973) [22] and Wang et al (2013) [8].

It is worth to note that many of the authors do not make an explicit distinction between gravity-shear waves of the KHBs type and propagating IGWs, and sometimes it is not clear

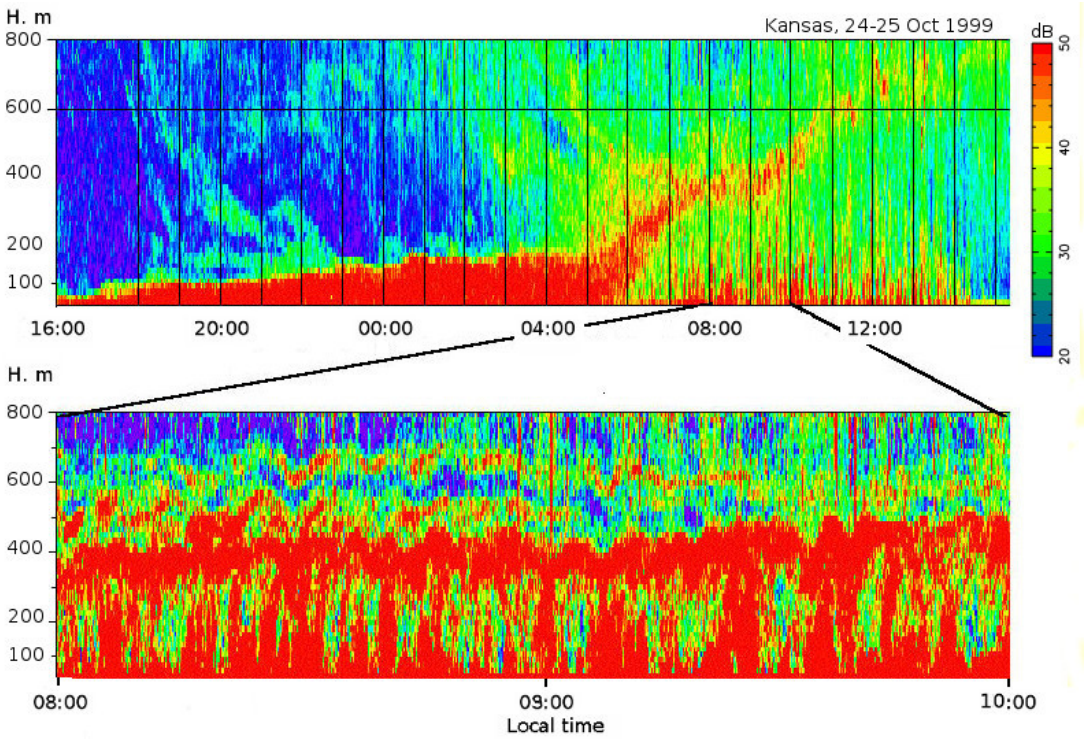


(a)

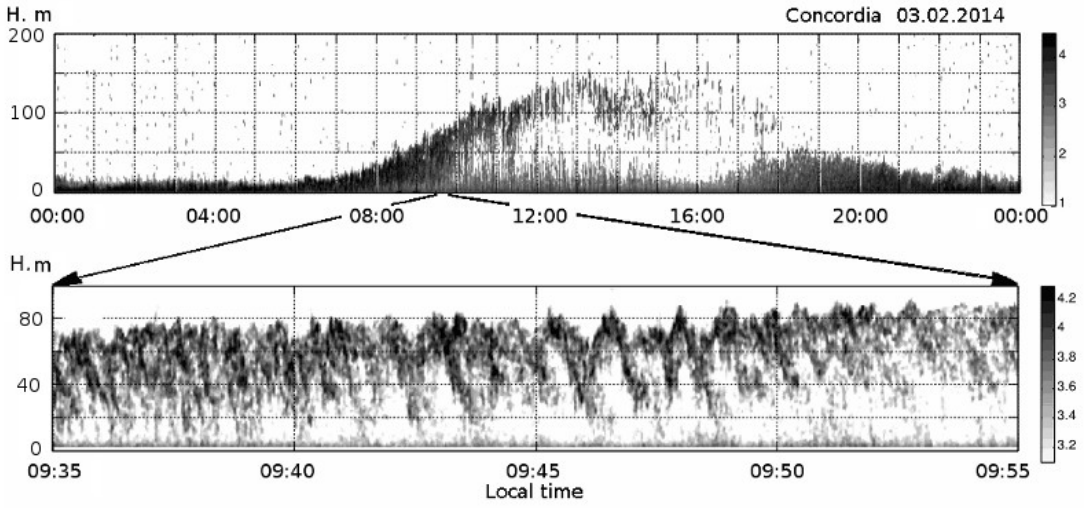


(b)

**Figure 2.** Examples of sodar visualization of KHBs within elevating inversion layers. Below of each echogram is shown its close-up with undulation pattern during morning development of the convective ABL. (a) Kansas, over the ABLE area during the CASES99 field study, 24-25 Oct 1999; sodar, f=1600 Hz (adapted from Coulter (2002) [10]). (b) Antarctic station Concordia, Dome C, 3 Feb 2014; SL high-resolution minisodar, f=4800 Hz (adapted from Petenko et al (2016) [11]).

**Table 1.** Number of KHBs episodes in 2011

| | Jan | Feb | Mar | Apr | May | June | July | Aug | Sept | Oct | Nov | Dec |
|---|---|---|---|---|---|---|---|---|---|---|---|---|
| Layers rising | 4 | 8 | 8 | 13 | 23 | 23 | 20 | 21 | 17 | 4 | 3 | 4 |
| KHBs rising | 3 | 6 | 1 | 2 | 13 | 9 | 11 | 10 | 7 | 2 | 0 | 0 |
| KHBs all | 10 | 10 | 1 | 2 | 13 | 9 | 12 | 12 | 8 | 3 | 2 | 3 |

what kind of waves they support one or other from the hypotheses. Meanwhile these two types of atmospheric waves have different shape, different temporal and spatial periods, different traveling speed, and evidently can have a different origin. Experimental data on differences in characteristics and behavior of these two kinds of the waves can be found in Petenko at al (2012) [23], Lyulyukin et al (2015) [24] and Kouznetsov et al (2016) [25].

## 3. Site and instrumentation

To analyze the KHBs during the morning transition the sodar data collected by the authors in 2011 were used. Round-the-year sodar measurements were carried out at the Zvenigorod Scientific Station (ZSS) of the A.M. Obukhov Institute of Atmospheric Physics, Russian Academy of Sciences (IAPh). The ZSS is located in a weakly inhomogeneous forestry terrain 45 km west of the Moscow city.

The three-axis Doppler sodar Latan-3 developed at the IAPh [26, 27] was continuously operated with a carrier frequency of 1700 Hz, a vertical resolution of 20 m, and the vertical range from 30 to 150-650 m, depending on noise level and weather. One sounding cycle is completed every 15 s. The sodar measurements of the intensity of return signal and wind velocity profiles were accompanied by measurements of the mean air temperature profiles with the help of a 60-MHz scanning radiometer MTP-5, developed at the Central Aerological Observatory, ATTEX, Russia [28]. The vertical resolution is 50 m, and the height range of sounding is from 20 m to 600 m. Besides, temperature and wind velocity were measured in situ by an ultrasonic thermometer-anemometer Metek USA-1 ("sonic" for short) installed in the top of 56-meter mast about 60 meters away from the sodar.

## 4. Results

A total of 148 cases of the morning lifting surface inversion layer were observed in 2011. This amount corresponds to the climatological mean number of cloudless and few cloudy days a year. Elevated inversion layers of other origins (for example, subsidence inversions or frontal inversions) were not taken into account. The total number of KHB trains such as "braids" that were identified in the echograms for the year amounted to 68 or about 45% of all cases of morning lifting. Monthly distribution of the number of such trains is shown in Table 1. In the 3-d raw of the table the total number of KHB episodes (in morning rising inversion layers and in nocturnal surface inversion layers) is indicated. It should be reminded that due to the limited temporal resolution of the sodar only braids with periods of more than one minute can be detected. A relatively small percentage of the detected KHBs cases can be connected with either the lack of temporal and vertical resolution of the sodar LATAN-3, or with the fact that many wave trains have limited horizontal sizes, hence only a small part of them are carried by the wind flow directly over the sodar.

The largest number of episodes observed in the summer months were associated with the morning rise of the inversions (but not with the nocturnal radiation inversions). This supports the assumption of a prominent role of convection in the formation of waves. But in reality, as will be shown below, it is not a "mechanical" impact of vertical convective motions, but the fact that a static stability in the rising inversion layer is lower than in the surface layer (because

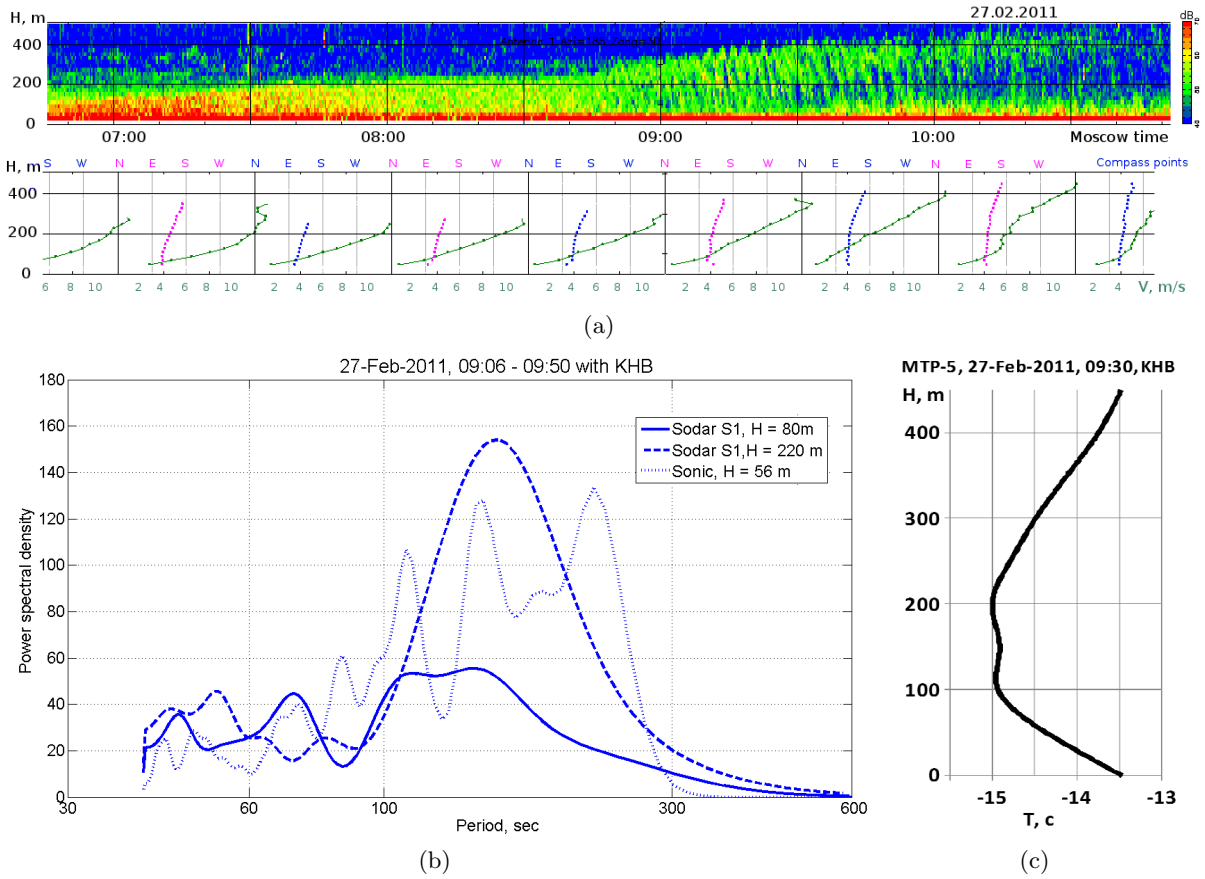


**Figure 3.** Features of the ABL parameters for KHBs episode Feb 27, 2011. (a) Sodar echogram of the ABL transition. Averaged over 30 minutes profiles of wind speed (green points) and direction (blue and pink points) measured by sodar are presented at the bottom of Figure 3a, directly under the echogram. (b) Power spectra of the intensity of the sodar at two heights: at the height of middle of a wavy layer and at the height of convective activity under the layer for the same interval of time. Besides, the power spectrum of temperature fluctuations measured by the sonic at the height of 56 m is plotted. (c) Profile of the 20-min averaged temperature by MTP-5.

temperature gradients and consequently the Richardson number are smaller), and therefore the conditions for the occurrence of shear instability ($Ri < 0.25$) are met better. But before we dwell on this fact, let us turn to the obtained spectra of the echo intensity.

The spectral analysis of the sodar return signal time series was used to estimate and compare the periods of the wavy structure in the rising inversion, and typical to periods of plume-shape convective structures beneath the rising inversion layers. Several low-frequency power spectra of the return signal from the wave layers for the most clear and longer trains were calculated. The power spectra were calculated using Welch's averaged, modified periodogram method of spectral estimation (see Welch 1967 [29])). Before the spectral processing, some filtering procedures were applied to reduce the noise impact and to extract the regular part of the undulation processes. All the spectra were then normalized by the variances of the time series. The heights of the time series of the return signal were chosen to be within the layer with wavy structures (usually near 200–250 m AGL). The spectra show peaks at the periods similar to those estimated earlier visually from the echograms.

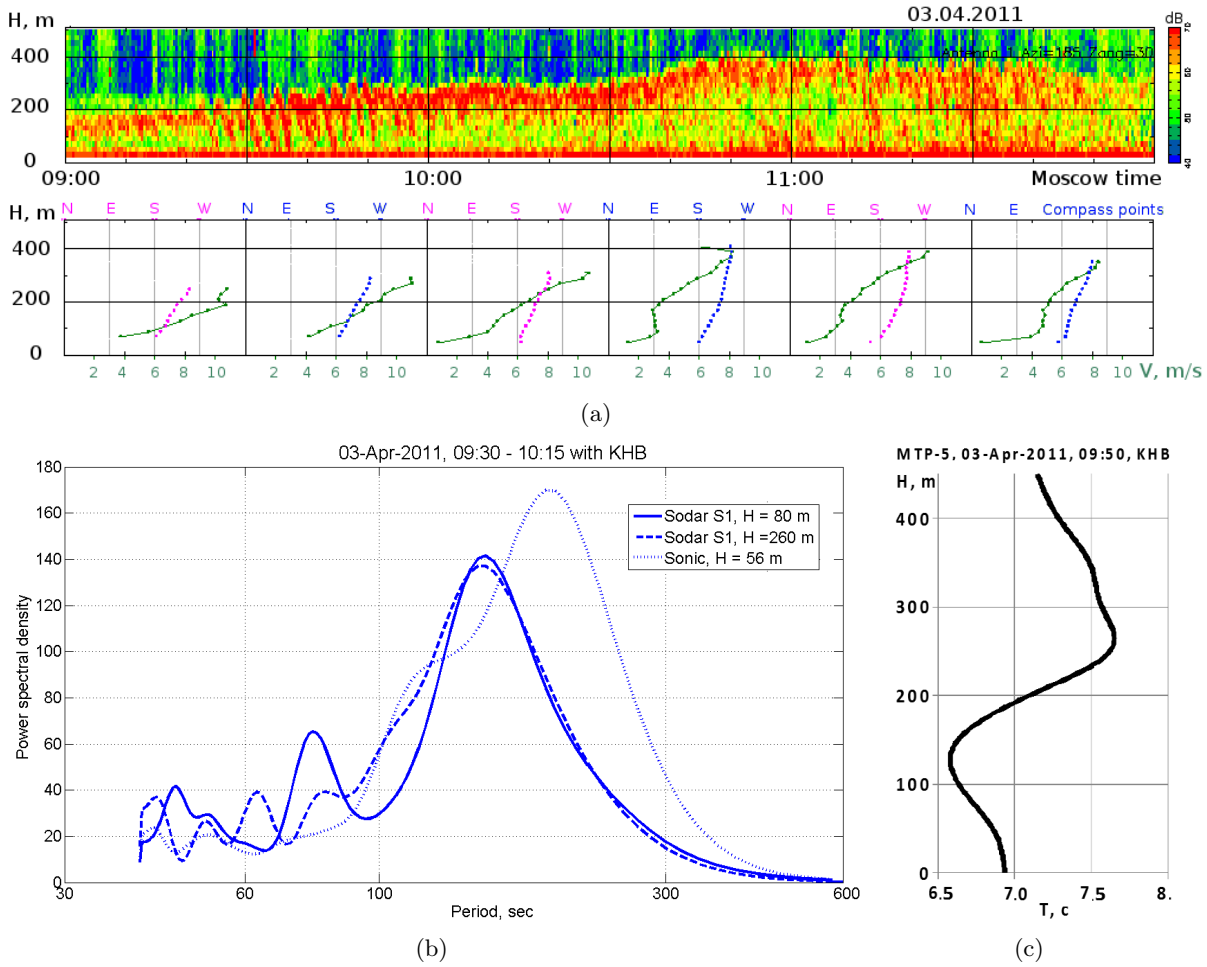


**Figure 4.** The same as in Fig. 3 for the KHBs episode of Apr 3, 2011.

Echograms visualizing the shape of the observed waves, and averaged profiles of wind speed and direction measured by sodar, are presented together with the spectra on Figs. 3 and 4. In Figure 3 an example of the KHB train obtained at ZSS in the winter season, Feb 27 2011, is shown. Clear wavy structures are seen in the plot of the return signal intensity in height-time coordinates (hereafter the sodar echogram) placed in the upper panel of Fig. 3(a). Backscattering of sound occurs at small-scale turbulent temperature inhomogeneities (with dimensions $l$ equal to half the wavelength of the sodar acoustic emission, $l \approx 10$ cm), and the intensity of the return signal is directly proportional to the temperature structural parameter $C_T^2$. Therefore, the sodar echogram presented on Figs. 3(a) shows the mesoscale wave motions in the field of smallscale temperature fluctuations. The train of waves exists within a morning rising inversion layer from 09:00 to 10:00 of local time. A plume-like shape of the signal beneath the waves evidences for developing of a weak convection near the surface. The bottom panel of Fig. 3(a) shows 30-minutes profiles of wind speed and direction. A magnitude of the wind shear reaches 4 m/s per 100 m.

Figure 3(b) contains 3 power spectra:

1) power spectrum of the time series of the return signal from a height of 200–300 m in the middle of rising layer;
2) power spectrum of the time series of the return signal from a height of several tens of meters

corresponding to the area of the surface convection occurrence;

3) power spectrum of the time series of temperature fluctuations at the height 56 meters according to sonic thermometer-anemometer mounted on the top of meteorological mast at a distance of 50 m from the sodar.

Temperature profile, measured with a scanning radiometer MTP-5 and averaged over the time interval for which the spectral density is calculated, are presented on Figures 3(c). It shows the temperature inversion ($dT/dz \sim 0.75°/100m$) in the rising layer, and unstable stratification near the surface. Comparison of the profile with the echogram pattern confirms a correctness of the echogram interpretation.

Figure 4 show the similar episode of KHB train in the morning rising layer, in spring, Apr 03 2011, at 09:20–10:10 of local time.

The results of the all used measurements presented in the Fig. 3 and Fig. 4 give information about the characteristic features of the phenomenon. Temperature profiles comply with the echogram pattern and show a stable stratification in the rising inversion layer, with a region of unstable stratification beneath, corresponding to the plume-shape nature of the echo signal with convection. Wind speed profiles show the rise of LLJ axis together with the raising of the inversion layer. Dominant spectral density peak (in dependence on the oscillation period) corresponds to the quasi-period of braids, visually estimated from the echograms.

Note that selection of time and height intervals to calculate the spectra was based on visual evaluation of the wave layer location from the echogram, and is therefore highly subjective. Since the oscillations are neither stationary nor strictly periodic, a slight shift of the echogram section (vertical or horizontal) selected for the calculation of the spectrum can lead to a shift in the position and intensity of the dominant peaks of the spectral density. Estimation of the possible errors is of great complexity. Therefore, a comparison of the positions of the peaks is more qualitative than quantitative.

Dominant periods in the spectra of the braids are equal to 120-150 sec. This corresponds to a frequency of 0.0067–0.0083 Hz, which exceeds the Brunt-Väisälä frequency $N_{B-V} = [(g/\theta)d\theta/dz]^{0.5}$, providing a value in these cases within the range 0.0018–0.0023 Hz. This indicates that the braids were not due to trapped gravity waves, which would have required $N_1 < f < N_2$ [17].

Estimates of the $Ri$ number value and the ratio between wavelength and double amplitude (i.e. wave layer thickness), $L_W/\Delta H$ were made. Braids are observed mostly with the wind speed V $\sim$ 12–16 m/s at the upper boundary of the rising layer and V $\sim$ 6–8 m/s in the middle of the layer. In this case wind shear in the layer reaches 4–5 m/s per 100 m, and the value of the Richardson number is

$$Ri = (g/\theta)\frac{(d\theta/dz)}{(dV/dz)^2} = 0.13 \div 0.21 < Ri_{crit} = 0.25,$$

i.e. static stability in the layers rising above the convection is not as strong as in the nocturnal surface inversions (where the vertical temperature gradient is often so large that it does not allow a dynamic shear instability to develop). Thus, the Kelvin-Helmholtz instability is the most likely source of the braids.

A rough estimate of the hypothesis of Taylor frozen turbulence under aforesaid wind speed 6–8 m/s suggests the magnitude of the braids spatial periods (i.e. wavelengths) $L_W \sim$ 750–1200 m. A typical layer thickness observing at ZSS $\Delta H \sim$ 200 m (in a time interval where the braids are clearly visible) gives the ratio $L_W/\Delta H \sim$ 4–5, which is close to the theoretical value for Kelvin-Helmholtz instability (on the Miles-Howard semicircle theorem). Dominant periods of the plume-shaped convective structures in the spectra are larger – about 200–240 sec. However, the wind speed at the heights of developing convective plumes is lower – about 3–4 m/s, that

leads to the similar estimates of the spatial periods of the plumes $L_P \sim$ 600–1000 m. Hence, the excitation of the braids by the convective activity beneath the capped inversion cannot be excluded.

Thus, the analysis of the power spectra of the braid structures and the plumes structures beneath, and of the synchronous data on wind speed and temperature profile, (and visualization of the patterns of the phenomena in the echograms) allow us to reject the hypothesis that the braids generation resulted from the passage, at relatively high speeds, of mesoscale waves, which perturbed the stability of the very nearly unstable boundary-layer shear flow in the course of their propagation (hypothesis A above) or that it is ducted orographic waves (hypothesis B above). However, this complex of measurement and calculation doesn't give the ground to distinguish between two other possible sources of the waves in the morning rising layers: Kelvin-Helmholtz instability (hypothesis C above) and convective activity underneath the layer.

It is worth to mention that power spectra obtained by Petenko and Bezverkhnii (1999) [30] under condition of developed free convection in the middle of summer days show the dominant frequencies close to the $N_{B-V}$ for the troposphere.

## 5. Conclusion

The data on the spectra in the transitional period suggests that the processes of wave and convective activity are linked. For a valid opinion which process is primary and which is secondary, more extensive statistical data on the spectra and profiles of mean wind speed and temperature are required. However, given the fact that in the rising morning inversion layers the necessary for shear instability development condition $Ri < 0.25$ was found, the most probable is the following process: KHBs type gravitational shear waves formed in the layer stimulate the development of the thermals. Note, that it was shown in [30] that predominant periods of about 7–9 minutes in the spectra of ABL parameters observed under conditions of developed convection can be due to the influence of the upper stable tropospheric layer which modulates convective processes in the ABL through the buoyancy wave activity with the Brunt-Väisälä frequency. Such a suggestion makes possible to combine hypotheses A and B into one.

*Acknowledgments*

This study was supported by the Russian Foundation for Basic Research, grants No 16-05-01072 and 16-05-00704. Data analysis and processing was supported by the Russian Science Foundation, grant No 14-27-00134.

## References

[1] Batchvarova E and Gryning S E 1994 *Bound.-Layer Meteor.* **71** 311–23
[2] Petenko I V 1996 *Proceed. ISARS'96* (27-31 May 1996, Moscow, Russia) pp 6.35–6.40
[3] Angevine W M and Baltink H K 2001 *Bound.-Layer Meteor.* **101**
[4] Lapworth A J 2006 *Bound.-Layer Meteor.* **119** 501–26
[5] Atlas D, Metcalf J I, Richter J H and Gossard E E 1970 *J. Atmos. Sci.* **27** 903–13
[6] McAllister L G, Pollard J R, Mahoney A R and Shaw P J R 1969 *Proced. IEEE* **57** 579–87
[7] Gibert F, Arnault N, Cuesta J, Plougonven R and Flamant P H 2011 *Q. J. R. Meteorol. Soc.* **137** 1610–24
[8] Wang Y, Creegan E, Felton M, Ligon D and Huynh G 2013 *J. Appl. Remote Sens.* **7** paper 073487
[9] Odintsov S L 2002 *Proceed. ISARS'2002* (24-28 June 2002, Rome, Italy) pp 271–74
[10] Coulter R L 2002 *Proceed. ISARS'2002, 24-28 June 2002, Rome, Italy* 321–29
[11] Petenko I, Argentini S, Casasanta G, Kallistratova M, Sozzi R and Angelo Viola A 2016 *Bound.-Layer Meteor. [in print]*
[12] Bean B R, McGavin R E, Chadwick R B and Warner B D 1971 *Bound.-Layer Meteor.* **1** 466–73
[13] Beran D W, Hooke W H and Clifford S F 1973 *Bound.-Layer Meteor.* **4** 133–53
[14] Deardorff J W 1969 *Phys. Fluids* **12 Suppl. II** 184–94
[15] Gossard E E, Jensen D R and Richter J H 1971 *J. of the Atmospheric Scienses* **28** 794–807
[16] Tennekes H 1973 *J. Atmos. Sci.* **30** 558–67

[17] Browning K A, Starr J R and Whyman A J 1973 *Bound.-Layer Meteor.* **4** 91–111
[18] Fochesatto G, Drobinski P, Flamant C, Guedalia D, Sarrat C, Flamant P H and Pelon J 2001 *Bound.-Layer Meteor.* **99** 451–64
[19] Chimonas G 1972 *Bound.-Layer Meteor.* **2** 444–52
[20] Hooke W H and Hall F F 1973 *Bound.-Layer Meteor.* **5** 29–41
[21] Chimonas G 1999 *Bound.-Layer Meteor.* **90** 397–421
[22] Reading C J, Golton E and Browning K A 1973 *Bound.-Layer Meteor.* **4** 275–87
[23] Petenko I, Mastrantonio G, Viola A, Argentini S and Pietroni I 2012 *Bound.-Layer Meteor.* **143** 125–41
[24] Lyulyukin V S, Kallistratova M A, Kouznetsov R D, Kuznetsov D D, Chunchuzov I P and Chirokova G Y 2015 *Izvestia, Atmos. Oceanic. Phys.* **51**[**2**] 193–202
[25] Kouznetsov R, Tisler P, Vihma T and Kallistratova M 2016 *Presentation at ISARS'2016* (Varna, Bulgary)
[26] Kouznetsov R D 2006 *Proceed. ISARS'2006* (18-20 July 2006, Garmisch-Partenkirchen, Germany) pp 97–98
[27] Kouznetsov R D, Kramar V F and Kallistratova M A 2007 *Meteorologische Zeitschrift* **16** 367–373
[28] Kadygrov E N, Shur G N and Viazankin A S 2003 *Radio Sci.* **38** 13.1–13.12
[29] Welch P D 1967 *IEEE Transactions on Audio Electroacoustics* **AU-15** 70–3
[30] Petenko I V and Bezverkhnii V A 1999 *Meteorol. Atmos. Phys.* **71** 105–16